

## Confirmation of a new resonance in $^{26}\text{Si}$ and contribution of classical novae to the galactic abundance of $^{26}\text{Al}$

L. Canete,<sup>1,\*</sup> D. T. Doherty<sup>1</sup>, G. Lotay,<sup>1</sup> D. Seweryniak,<sup>2</sup> C. M. Campbell,<sup>3</sup> M. P. Carpenter,<sup>2</sup> W. N. Catford,<sup>1</sup> K. A. Chipps,<sup>4</sup> J. Henderson,<sup>1</sup> R. G. Izzard,<sup>1</sup> R. V. F. Janssens<sup>5,6</sup>, H. Jayatissa,<sup>2</sup> J. José,<sup>7,8</sup> A. R. L. Kennington,<sup>1</sup> F. G. Kondev,<sup>2</sup> A. Korichi,<sup>2,9</sup> T. Lauritsen,<sup>2</sup> C. Müller-Gatermann,<sup>2</sup> C. Paxman,<sup>1</sup> Zs. Podolyák,<sup>1</sup> B. J. Reed,<sup>1</sup> P. H. Regan,<sup>1,10</sup> W. Reviol,<sup>2</sup> M. Siciliano,<sup>2</sup> G. L. Wilson,<sup>2,11</sup> R. Yates,<sup>1</sup> and S. Zhu<sup>12,†</sup>

<sup>1</sup>*School of Mathematics and Physics, University of Surrey, Guildford GU2 7XH, United Kingdom*

<sup>2</sup>*Physics Division, Argonne National Laboratory, Argonne, Illinois 60439, USA*

<sup>3</sup>*Nuclear Science Division, Lawrence Berkeley National Laboratory, Berkeley, California 94720, USA*

<sup>4</sup>*Oak Ridge National Laboratory, Oak Ridge, Tennessee 37831, USA*

<sup>5</sup>*Department of Physics, University of North Carolina at Chapel Hill, Chapel Hill, North Carolina 27599, USA*

<sup>6</sup>*Triangle Universities Nuclear Laboratory, Duke University, Durham, North Carolina 27708, USA*

<sup>7</sup>*Departament de Física, Universitat Politècnica de Catalunya, Barcelona E-08019, Spain*

<sup>8</sup>*Institut d'Estudis Espacials de Catalunya (IEEC), E-08034 Barcelona, Spain*

<sup>9</sup>*Laboratoire de Physique des 2 Infinis Irène Joliot-Curie, CNRS/IN2P3, Université Paris-Saclay, Orsay, France*

<sup>10</sup>*National Physical Laboratory, Teddington TW11 0LW, United Kingdom*

<sup>11</sup>*Louisiana State University, Baton Rouge, Louisiana 70803, USA*

<sup>12</sup>*Brookhaven National Laboratory, National Nuclear Data Center, Upton, New York 11973, USA*



(Received 8 September 2022; revised 2 June 2023; accepted 18 August 2023; published 14 September 2023)

The  $^{25}\text{Al}(p, \gamma)$  reaction has long been highlighted as a possible means to bypass the production of  $^{26}\text{Al}$  cosmic  $\gamma$  rays in classical nova explosions. However, uncertainties in the properties of key resonant states in  $^{26}\text{Si}$  have hindered our ability to accurately model the influence of this reaction in such environments. We report on a detailed  $\gamma$ -ray spectroscopy study of  $^{26}\text{Si}$  and present evidence for the existence of a new, likely  $\ell = 1$ , resonance in the  $^{25}\text{Al} + p$  system at  $E_r = 153.9(15)$  keV. This state is now expected to provide the dominant contribution to the  $^{25}\text{Al}(p, \gamma)$  stellar reaction rate over the temperature range,  $T \approx 0.1\text{--}0.2$  GK. Despite a significant increase in the rate at low temperatures, we find that the final ejected abundance of  $^{26}\text{Al}$  from classical novae remains largely unaffected even if the reaction rate is artificially increased by a factor of 10. Based on new, galactic chemical evolution calculations, we estimate that the maximum contribution of novae to the observed galactic abundance of  $^{26}\text{Al}$  is  $\approx 0.2M_{\odot}$ . Finally, we briefly highlight the important role that super-asymptotic giant branch stars may play in the production of  $^{26}\text{Al}$ .

DOI: [10.1103/PhysRevC.108.035807](https://doi.org/10.1103/PhysRevC.108.035807)

### I. INTRODUCTION

The presence of large  $^{26}\text{Mg}$  anomalies attributed to the decay of  $^{26}\text{Al}$  ( $t_{1/2} = 7.2 \times 10^5$  yr) in calcium-, aluminium-rich inclusions (CAIs) represents a particularly striking feature of our solar system [1]. CAIs were the first meteoritic solids to form in the solar protoplanetary disk and, as such, it is likely that live  $^{26}\text{Al}$  was injected into the solar system at the beginning of its existence. In particular, while the solar system was endowed with a wide variety of short-lived

radionuclides [2], it is thought that due to the large amount of energy released in its decay,  $^{26}\text{Al}$  provided the main source of heat for the earliest planetesimals and planetary embryos. Moreover, in melting the icy layers of planetesimals,  $^{26}\text{Al}$  may have played a key role in determining the bulk water fraction of terrestrial planets, which constitutes an essential ingredient for establishing their habitability [3]. Consequently, ever since its initial discovery in the Allende meteorite in the 1976 [1], determining the exact stellar origin of  $^{26}\text{Al}$  has been the focus of extensive theoretical and experimental efforts.

In more recent years, it has become possible to study the galactic distribution of  $^{26}\text{Al}$  via space-based observations of its characteristic 1.809-MeV decay  $\gamma$  rays [4–7]. The COMPTEL and INTEGRAL satellite missions have constrained the active galactic abundance of  $^{26}\text{Al}$  to lie in the range 1.7–3.5  $M_{\odot}$  [6,7], with the best current estimate of 2.0  $M_{\odot}$  [8], and have localized the emission of cosmic  $\gamma$  rays to well-known star-forming regions [9]. As such, it is likely that  $^{26}\text{Al}$  is predominantly distributed throughout the interstellar medium by

\*l.canete@surrey.ac.uk

†Deceased.

Published by the American Physical Society under the terms of the [Creative Commons Attribution 4.0 International](https://creativecommons.org/licenses/by/4.0/) license. Further distribution of this work must maintain attribution to the author(s) and the published article's title, journal citation, and DOI.

massive stars, either during core collapse via explosive Ne/C burning, or by violent stellar winds during the preceding Wolf-Rayet phase [10]. However, a number of additional sources, including classical novae and asymptotic giant branch (AGB) stars, may still contribute considerably to the overall galactic budget of  $^{26}\text{Al}$ . Therefore, it is important that these be investigated to fully account for the 1.809-MeV line intensity. While classical novae and AGB stars are efficient producers of  $^{26}\text{Al}$  [11,12], the probability of associating such environments with star-forming regions is expected to be relatively low [13]. It has been suggested that super AGB (SAGB) could achieve temperatures at the base of their envelopes of  $\approx 0.16$  GK [14] meaning that proton-capture reactions involving heavier species may become important for understanding the nucleosynthesis in these environments.

In classical novae, the following expression provides a crude estimate for the maximum contribution of such scenarios to the galactic abundance of  $^{26}\text{Al}$  [11,15],

$$M(^{26}\text{Al}) \approx \tau(^{26}\text{Al})f_{\text{ONe}}M_{\text{ej}}X(^{26}\text{Al})R_{\text{nova}}. \quad (1)$$

Here,  $X(^{26}\text{Al})$  is the mean mass fraction of  $^{26}\text{Al}$  in the ejecta,  $f_{\text{ONe}}$  is the fraction of novae that have oxygen-neon white dwarfs (typically  $\approx 1/3$  [16,17]),  $M_{\text{ej}}$  is the mass ejected in an outburst,  $R_{\text{nova}}$  is the nova rate in our galaxy ( $\approx 50_{-23}^{+31}$  yr $^{-1}$  [18]) and  $\tau(^{26}\text{Al})$  is the mean lifetime of  $^{26}\text{Al}$  ground state (1.04 Myr). When using the above expression, a range of masses from 0.1–0.6  $M_{\odot}$  have previously been computed for the contribution of classical novae to the overall galactic abundance of  $^{26}\text{Al}$  [11,19,20]. Reference [19] claims that classical novae may be responsible for up to 30% of  $^{26}\text{Al}$  in our galaxy, which, depending on the total abundance observed, could be as large as  $\approx 1 M_{\odot}$ . These variations likely stem from uncertainties in the underlying nuclear physics processes governing the production of  $^{26}\text{Al}$  and hence, it is essential that such uncertainties be reduced in order to accurately estimate the role of classical novae in the production of cosmic  $\gamma$  rays throughout the galaxy. Moreover, in constraining uncertainties relating to  $^{26}\text{Al}$  nucleosynthesis in classical nova events, it may be possible to uniquely assign the astrophysical origin of some presolar grains. These microscopic pieces of matter are characterized by large isotopic anomalies that can only be explained by the nuclear processes that took place in the parent star around which they form, and, recently, several grains have been identified with high  $^{26}\text{Al}/^{27}\text{Al}$  ratios [21–24].

In this regard, one of the key remaining uncertainties in  $^{26}\text{Al}$  nucleosynthesis relates to the extent to which the  $^{25}\text{Al}(p, \gamma)^{26}\text{Si}$  reaction bypasses the flow of material from the  $^{25}\text{Mg}(p, \gamma)^{26}\text{Al}(p, \gamma)^{27}\text{Si}$  capture sequence [25–28] at high temperatures. The former circumvents the production of the  $^{26}\text{Al}$  ground state and results in sole population of the isomeric level at  $E_x = 228$  keV ( $t_{1/2} = 6.3$  s). This excited-isomeric state undergoes a superallowed  $\beta^+$  decay directly to the  $^{26}\text{Mg}$  ground state and, as such, reduces the flux of 1.809-MeV cosmic  $\gamma$  rays from novae.

Over the peak temperature range of nuclear burning in classical novae ( $T \approx 0.1$ – $0.4$  GK), the  $^{25}\text{Al}(p, \gamma)$  reaction is expected to be dominated by resonant capture to excited states in  $^{26}\text{Si}$  [19,20,29–40] above the proton-emission

threshold energy of 5513.99(13) keV [41]. In particular, a  $3_3^+$  excited state at  $E_x = 5927.6(10)$  keV in  $^{26}\text{Si}$ , corresponding to an  $\ell = 0$  resonance at  $E_r = 413.6(10)$  keV in the  $^{25}\text{Al} + p$  system, is expected to make the most significant contribution to the stellar reaction rate for  $T > 0.2$  GK. The proton and  $\gamma$ -ray partial widths of this state have been experimentally measured to be  $\Gamma_p = 2.9(10)$  eV [32] and  $\Gamma_\gamma = 40 \pm 11(\text{stat.})_{-18}^{+19}(\text{lit.})$  meV [19], respectively—the latter uncertainty in  $\Gamma_\gamma$  reflects the use of literature data for the  $\beta$ -decay branches of  $^{26}\text{P}$ . Furthermore, the 5928-keV level in  $^{26}\text{Si}$  is uniquely paired with an analog  $3_3^+$  state at 6125.3(3) keV in the mirror nucleus,  $^{26}\text{Mg}$  [42]. In adopting the neutron spectroscopic factor of the 6125-keV excited state in  $^{26}\text{Mg}$  [20,39] to estimate the proton-partial width, one obtains 4.0(12) eV in good agreement with Ref. [32]. Similarly, a recent measurement of the lifetime of the 6125-keV level in  $^{26}\text{Mg}$  of 19(3) fs [20] leads to a  $\gamma$ -ray partial width of 33(5) meV in accord with Ref. [19]. Additional contributions to the  $^{25}\text{Al}(p, \gamma)$  reaction are expected at lower temperatures ( $< 0.2$  GK) from excited states at 5675.2(14) and 5890.0(8) keV in  $^{26}\text{Si}$  [37]. These are assigned as  $1_1^+$  and  $0_4^+$  levels [36,40], respectively, and their strengths estimated from properties of their well-matched mirror analogs in  $^{26}\text{Mg}$  at 5691.1(2) and 6255.5(1) keV. Consequently, uncertainties related to the resonant properties of excited states at 5676, 5890, and 5928 keV in  $^{26}\text{Si}$  are now reasonably well constrained. However, in recent work, combining data from complementary  $^{11}\text{B}(^{16}\text{O}, p)^{26}\text{Mg}$  fusion-evaporation and  $^{25}\text{Mg}(d, p)^{26}\text{Mg}$  transfer-reaction studies, a previously unobserved  $1_1^-$  level was newly identified in  $^{26}\text{Mg}$  at an excitation energy of 5710.0(36) keV [20]. This level was tentatively matched to an analog state in  $^{26}\text{Si}$  at 5949.7(40) keV in Ref. [20], as it appeared to be the only available excited state in  $^{26}\text{Si}$  in a reasonable energy range without a unique spin-parity assignment. However, questions have been raised over the existence of a state at 5946 keV which was reported by Parpottas *et al.* using the  $^{24}\text{Mg}(^3\text{He}, n)$  reaction [30] but was not observed in more recent experiments (e.g., [36,40]) and, as such, the exact location of the  $1_1^-$  analog in  $^{26}\text{Si}$  remains unknown.

However, based on known Coulomb-energy differences in the  $T = 1, A = 26$  mirror system, the lowest-lying  $1_1^-$  excited state in  $^{26}\text{Si}$  should lie in the region of interest for explosive hydrogen burning in classical novae and, depending on its precise location, could significantly increase the astrophysical reaction rate. To date, shell-model predictions for  $^{26}\text{Si}$  have focused only on positive-parity states, see Ref. [35], so we, therefore, perform new calculations for this work with the code NUSHELLX utilizing the SPDF interaction [43] to investigate negative-parity levels. These calculations predict that the primary decay mode of the  $1_1^-$  level is a high-energy  $E1$  transition directly to the ground state.

Here, we present a new, precision  $\gamma$ -ray spectroscopy study of  $^{26}\text{Si}$  that exploits the unique capabilities afforded by the experimental coupling of the GRETINA tracking array and the Argonne Fragment Mass Analyzer (FMA) [44,45]. Specifically, the high efficiency and excellent Doppler reconstruction for high-energy  $\gamma$  rays of GRETINA, together with the rigorous channel selectivity provided by the FMA, allows for

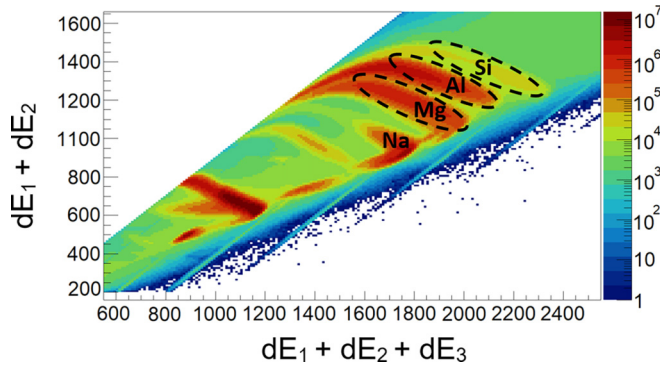


FIG. 1. A typical  $\Delta E$ - $E$  ionization chamber histogram used for  $Z$  selectivity. The distinct regions associated with various atomic numbers are labeled. Example software particle identification gates are shown on the histogram.

the observation of several new, previously unreported, high-energy, ground-state transitions in  $^{26}\text{Si}$ , including a likely candidate for the proposed  $1_1^-$  resonance [20].

## II. EXPERIMENTAL DETAILS

The experiment was performed at Argonne National Laboratory's ATLAS facility, where a 50 pA, 68-MeV beam of  $^{16}\text{O}$  ions bombarded a  $\approx 200 \mu\text{g}/\text{cm}^2$ -thick  $^{12}\text{C}$  target for  $\approx 104$  h, producing  $^{26}\text{Si}$  nuclei via the  $^{12}\text{C}(^{16}\text{O}, 2n)$  fusion-evaporation reaction. Prompt  $\gamma$  rays were detected with the GREINA tracking array [46,47], which consisted of 12 modules of 4 HPGe crystals, in coincidence with recoiling reaction products, registered at the focal plane of the FMA [48] specifically set for the mass to charge state,  $A/Q$ , of 26/10. This charge state was chosen to maximize the yield for the recoils of interest at the focal plane. The focal plane position was determined with a position-sensitive parallel-grid avalanche counter (PGAC), with position slits also used to block unwanted species at the focal plane such as  $A/Q = 27/10$  recoils. A segmented ionization chamber was used to separate Si, Al, and Mg nuclei through their  $\Delta E$ - $E$  information (Fig. 1). Standard  $^{88}\text{Y}$ ,  $^{56}\text{Co}$ , and  $^{152}\text{Eu}$  sources were used for energy and efficiency calibrations, while an additional 6.129-MeV  $\gamma$ -ray transition in  $^{16}\text{O}$ , following  $^{13}\text{C}(\alpha, n)$  reactions, was used to refine the GREINA energy calibration at high energies. In these measurements a 9-keV FWHM was obtained for the 6.129-MeV peak. Identical  $\gamma$ -ray tracking conditions were used for the calibration and in-beam data. Clean  $\gamma$ -ray singles spectra and  $\gamma$ - $\gamma$  coincidence matrices were produced and analyzed by applying appropriate conditions on the energy-loss information and  $A/Q$  parameter determined with the detectors of the FMA focal plane. Table I summarizes the properties of the observed excited states in  $^{26}\text{Si}$  in comparison with previous work. Figure 2 displays the total tracked and Doppler-corrected  $\gamma$ -ray singles spectrum detected in coincidence with  $^{26}\text{Si}$  recoils while an example  $\gamma$ - $\gamma$  coincidence spectrum, gated on the 989-keV  $2_2^+ \rightarrow 2_1^+$  transition is shown in Fig. 3. The uncertainties on the  $\gamma$ -ray energies in Table I include both the statistical uncertainty

TABLE I. Properties of excited states in  $^{26}\text{Si}$ . Previous excitation energies and spin-parity assignments have been taken from Ref. [42]. The level energies are corrected for the recoil of the compound nucleus. If more than one  $\gamma$ -decay branch is observed to depopulate a state the derived excitation energy ( $E_x$ ) corresponds to a weighted average.

$E_x$ [keV] previous	$E_x$ [keV] present	$E_\gamma$ [keV]	$I_\gamma$ [%]	$J^\pi$
1797.3(1)	1797.2(1)	1797.1(1)	100	$2_1^+$
2787.1(1)	2786.2(1)	988.9(1)	28.0(2)	$2_2^+$
		2786.2(1)	13.6(5)	
3336.4(2)	3336.6(10)	1539.3(10)	2.1(2)	$0_2^+$
3757.6(2)	3757.4(1)	970.8(1)	7.1(1)	$3_1^+$
		1960.1(1)	11.0(2)	
4139.1(2)	4139.3(3)	1352.2(4)	0.5(2)	$2_3^+$
		2342.1(2)	5.1(2)	
		4138.4(5)	0.6(1)	
4187.8(2)	4187.2(3)	1400.1(2)	11.3(2)	$3_2^+$
		2389.9(2)	4.9(3)	
4446.4(2)	4446.4(1)	1659(2)	0.5(1)	$4_1^+$
		2649.1(1)	19.4(2)	
4796.9(8)	4796.2(2)	2998.8(2)	14.3(2)	$4_2^+$
4811.0(10)	4811.4(4)	2025.2(4)	5.5(1)	$2_4^+$
4831.2(4)	4831.3(20)	2045(2)	1.1(3)	$0_3^+$
5147.5(8)	5147.5(7)	2359.9(5)	3.5(2)	$2_5^+$
		5147.1(9) <sup>a</sup>	0.7(2)	
5289.0(2)	5289.2(5)	842.5(3)	3.0(1)	$4_3^+$
		1532.3(2)	2.2(2)	
		2502(2)	0.3(2)	
		3491.5(10)	0.6(2)	
5517.8(2)	5516.8(7)	1071.6(2)	3.3(1)	$4_4^+$
		1329.5(3)	5.1(1)	
		1764(2)	3.3(3)	
		2735(2)	0.2(1)	
new state	5667.9(15)	5667.2(15) <sup>a</sup>	0.3(1)	$1_1^-$
5676.2(3)	5675.6(4)	2888.3(22)	0.2(1)	$1_1^+$
		3878.0(4)	1.3(3)	
5890.1(3)	5889.4(17)	4091.9(17)	0.4(2)	$0_4^+$

<sup>a</sup>Newly observed transition.

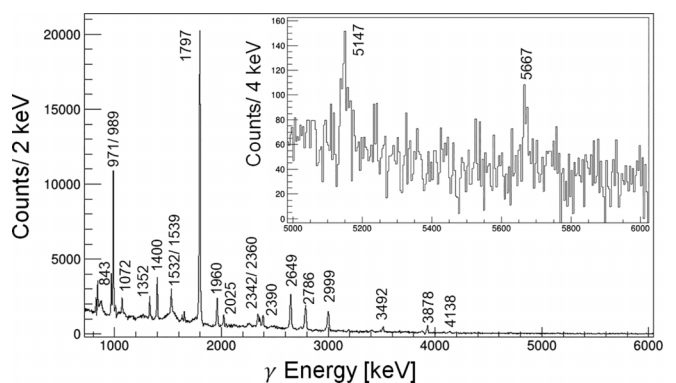


FIG. 2. Tracked and Doppler-corrected  $\gamma$ -ray energy spectrum measured in coincidence with  $^{26}\text{Si}$  recoils at the FMA focal plane. The inset shows the energy region of interest for high-energy direct-to-ground state decays.

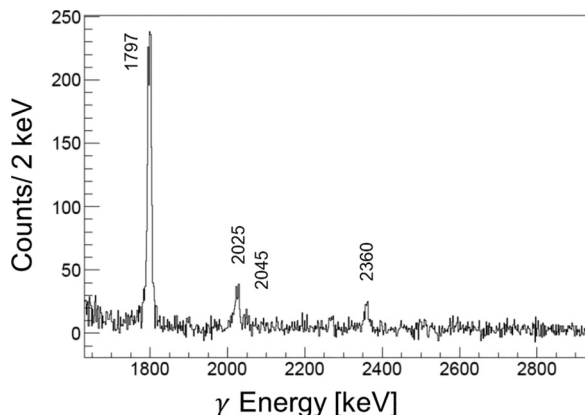


FIG. 3. A portion of the  $\gamma$ -ray spectrum gated on the 989-keV transition in  $^{26}\text{Si}$ . The energies of the  $\gamma$  rays are given in keV.

and a systematic uncertainty associated with the Doppler shift (deduced from the distribution of recoil velocities).

### III. RESULTS

Overall, good agreement is found between the present work and Ref. [42] for level energies and  $\gamma$ -decay branches of all states up to 6 MeV excitation energy. The key  $3_3^+$ , 5928-keV level, exhibits a dominant proton-decay branch which explains the nonobservation of the 1742-keV transition from this state in the present work. Moreover, only the most intense  $\gamma$  ray depopulating the  $0_4^+$  state was observed, which is consistent with the weak population expected for a  $0^+$  level in the heavy-ion fusion-evaporation mechanism. However, as shown in the inset of Fig. 2, we report the observation of two new, high-energy  $\gamma$  decays at 5147.1(9) and 5667.2(15) keV. The first of these corresponds to a hitherto unobserved direct-to-ground state decay branch from the known, particle bound,  $2_5^+$  level. The excitation energy derived from the newly observed direct-to-ground state transition agrees with that deduced by analyzing  $\gamma$ - $\gamma$  cascades (Table I) and with previous work [42]. On the other hand, the new 5667.2(15)-keV transition does not correspond to a previously identified level in  $^{26}\text{Si}$ .

#### A. GRETINA response to high-energy $\gamma$ rays

The two new  $^{26}\text{Si}$   $\gamma$  rays we report on (with energies of 5147 and 5667 keV) differ in energy by 520 keV. As can be seen in Table I the energy calibration is reliable for high-energy  $\gamma$  rays but, in order to eliminate the possibility of the 5147-keV peak corresponding to a single-escape peak, a GEANT4 Monte Carlo simulation was performed for the GRETINA array. In the simulation the response of the array to a single 5667-keV  $\gamma$  ray was investigated, as shown in Fig. 4. One observes a single-escape peak that is a factor of more than 3 less intense than its corresponding photo peak whereas the 5147-keV transition is observed to be more intense than the peak at 5667-keV in our data. This provides additional confidence that the newly reported transition at 5147-keV is indeed a new transition in  $^{26}\text{Si}$  and not a single escape peak. The simulation was bench marked with data from the

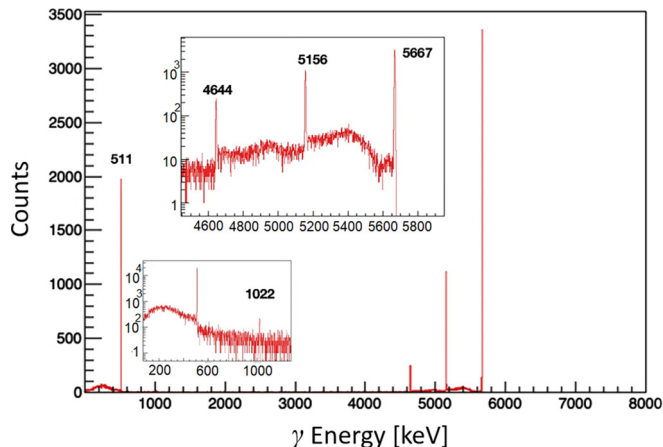


FIG. 4. A GRETINA energy spectrum simulated with the GEANT4 toolkit, displaying the response to an isolated 5667-keV  $\gamma$  ray. The insets show portions of the spectrum zoomed in on the single- and double-escape peaks and on region around 511 keV.

$^{16}\text{O}$  source, discussed previously, where a comparable FWHM was obtained for the 6.129-MeV transition.

#### B. Interpretation of the new 5667-keV transition

No  $\gamma$  rays were observed in coincidence with the newly reported 5667-keV transition in the  $\gamma$ - $\gamma$  coincidence analysis. However, if we consider the possibility that this transition does belong to a cascade in  $^{26}\text{Si}$ , with the coincident transition(s) not observed due to the  $\gamma$ -ray detector efficiency and collected statistics, then it would imply the existence of a state at an excitation energy of greater than 7.4 MeV (assuming that the state decayed to the  $2_1^+$  level at 1797 keV). The largest multipolarity that could be observed in an in-beam study of this type is  $E2$  which would imply a maximum spin-parity of  $4^+$  for a level feeding the  $2^+$  excitation. However, such a state would be particle unbound by almost 2 MeV and would, therefore, decay almost entirely by proton emission in contrast with the present observation of a  $\gamma$  ray.

This, therefore, suggests that the 5667-keV transition corresponds to a direct-to-ground state decay from a new state above the proton-emission threshold in  $^{26}\text{Si}$ . The 5667.9(15)-keV excitation energy implied by such a transition disagrees with that for any known  $^{26}\text{Si}$  state at the  $\approx 4\sigma$  level. Moreover, it should be noted that no such transition was reported in the recent measurement of Ref. [40], which gated on neutrons in coincidence with  $^{26}\text{Si}$ , and clearly observed all known decays from the nearby  $1_1^+$  5676-keV state. On the other hand, the proximity of this new state to the known 5676-keV level explains its nonobservation in previous particle transfer work, e.g., [29], while its spin and parity quantum numbers, which are discussed below, likely prohibit its population in experiments where  $^{26}\text{Si}$  levels are populated following the  $\beta$  decay of  $^{26}\text{P}$  [ $J^\pi = (3^+)$ ] [19].

#### C. Spectroscopic properties of the new $^{26}\text{Si}$ resonance

In an in-beam  $\gamma$ -ray study of this type only  $E1$ ,  $M1$ , and  $E2$  transitions are typically observed as higher-multipolarity



transitions are too slow to compete. This restricts the possible spin-parity quantum numbers of the new 5668-keV level to  $1^+$ ,  $1^-$ , or  $2^+$  due to the observation of a direct-to-ground state decay branch.

Based on shell-model calculations of excited states in  $^{26}\text{Si}$  over an excitation energy range  $E_x = 5\text{--}7$  MeV [49], only  $1^-$  levels are predicted to exhibit strong,  $\approx 90\%$   $\gamma$ -decay branches directly to the ground state. The next strongest branch ( $\approx 6\%$ ), to the  $0_2^+$  level was not observed in the current study due to the limited statistics obtained. In contrast, the nearby  $1_1^+$  state at 5676 keV is predicted to display a dominant decay path towards the  $2_1^+$  state, in agreement with experiment, with only a weak ( $\approx 6\%$ ) decay branch towards the ground state. Such a branch would correspond to a  $\gamma$ -ray intensity of  $<0.1$  and would not be observable in the present work. There are no remaining unassigned positive-parity levels in  $^{26}\text{Si}$  for  $E_x = 0\text{--}6$  MeV and the  $1_2^+$  and  $2_6^+$  states are not predicted to exist until  $\approx 6.6$  MeV [49]. The shell-model calculations in the present work are performed with the SPDPF interaction but calculations with other interactions yield the same conclusions for the  $1_1^-$  state, i.e., a dominant decay path towards the ground state.

This implies that the 5668-keV level is likely the mirror analog of the recently identified  $1_1^-$ , 5710-keV excited state in  $^{26}\text{Mg}$  [20]. In [20], the state was observed in a  $\gamma$ - $\gamma$ - $\gamma$  triples analysis through its decay to the  $0_2^+$  level. The Gammasphere trigger condition that was utilized in Ref. [20], which required at least two coincident  $\gamma$  rays, would not have permitted the observation of the direct-to-ground state decay, observed here for the  $1^-$  excitation, since such a nonyrast level would be fed very weakly by higher-lying states. Likewise, and as discussed above, the direct-to-ground state decay branch for a  $1_1^-$  level is predicted to be by far the dominant decay branch with the weak predicted decay to the  $0_2^+$  level in  $^{26}\text{Si}$ , which would result in a 2331-keV  $\gamma$  ray, being beyond the present experimental sensitivity owing to the use of the FMA for channel selectivity. To this end, we would encourage careful reanalysis of previous high-statistics  $^{26}\text{Si}$  data sets to search for the as yet unreported 2331-keV transition.

The  $1^-$  assignment for the 5668-keV state is further supported by examining the mirror-energy differences between  $^{26}\text{Si}$ - $^{26}\text{Mg}$  mirror pairs (Fig. 5). Matching the 5668-keV level with its counterpart in  $^{26}\text{Mg}$  state at an excitation energy of 5710 keV [20] implies a small mirror-energy difference of 42 keV whereas both the  $1_2^+$  and  $2_6^+$  possibilities would require significant mirror-energy shifts in contrast to those observed for other levels in the  $T = 1, A = 26$  system.

The possible 5946-keV level in  $^{26}\text{Si}$  is not included in Fig. 5 as its existence is not fully established. It should be noted, however, that, if this state does exist, it does not represent the best candidate for the  $1_1^-$  level as it would imply a mirror-energy difference of 236 keV which is larger than the shifts observed for other mirror pairs. Furthermore the direction of the shift, with the  $^{26}\text{Si}$  level being at higher excitation energy than its counterpart in  $^{26}\text{Mg}$ , would be opposite to the general trend observed in this system (as shown in Fig. 5).

Consequently, we conclude that the newly observed 5668-keV excited state in  $^{26}\text{Si}$  most likely represents the missing  $1_1^-$  level and thus corresponds to a new  $\ell = 1$  resonance

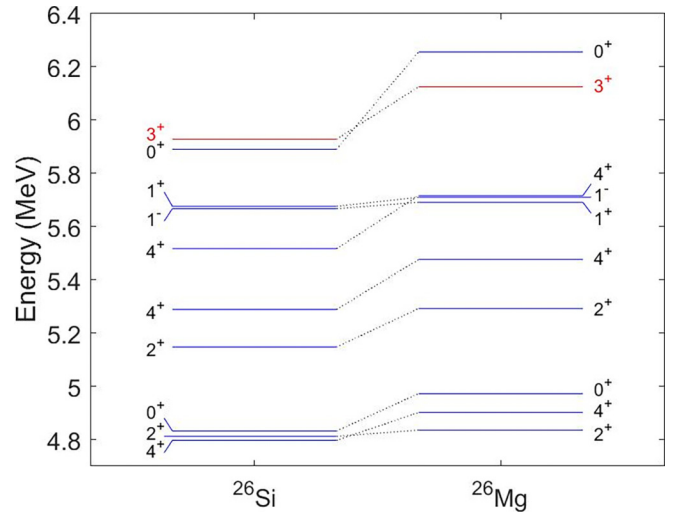


FIG. 5. Favored mirror assignments for excited states in  $^{26}\text{Si}$  (left) and  $^{26}\text{Mg}$  (right) between 4.5 and 6.4 MeV. The  $3^+$  state, which is labeled in red, is not observed in the current study but the mirror assignment has been well established in previous work.

in the  $^{25}\text{Al} + p$  system at  $E_r = 153.9(15)$  keV. However, as no angular-distribution analysis could be performed for the 5667-keV  $\gamma$  ray it is not possible to completely rule out  $1^+$  or  $2^+$  assignments for the 154-keV resonance, although both would imply very large mirror-energy differences which are not observed for other levels (Fig. 5). The only other odd-parity possibility is the  $3_1^-$  level which is predicted to exist at an energy of 6354 keV in our shell-model calculations, however, this possibility is definitively ruled out by the observation of a direct to ground-state decay branch.

A definitive spin-parity assignment for the new level at 5668 keV would, therefore, require further investigation which could include careful reanalysis of earlier particle transfer studies or new work combining high-resolution  $\gamma$ -ray spectroscopy with transfer reactions.

#### IV. ASTROPHYSICAL IMPLICATIONS

To evaluate the  $^{25}\text{Al}(p, \gamma)$  stellar-reaction rate, we consider the contribution of excited states in  $^{26}\text{Si}$  at 5667.9(15), 5676.2(3), 5890.1(3), 5927.6(10), and 5945.9(40) keV, corresponding to resonances at  $E_r = 153.9(15)$ , 162.2(4), 376.1(3), 413.6(10), and 431.9(40) keV, respectively. Table II summarizes the properties of resonances in the  $^{25}\text{Al}(p, \gamma)$  reaction. Gamma-ray partial widths,  $\Gamma_\gamma$ , are adopted from the published shell-model calculations [35], except for the 414-keV resonance where the experimental value of Bennett *et al.* [19] is used. We favor the  $\Gamma_\gamma$  of Ref. [19] for the 414-keV resonance rather than the more recent width of Ref. [38] as the latter has a larger uncertainty and disagrees with the value determined for the mirror-analog level in  $^{26}\text{Mg}$  [20]. To estimate the proton partial widths,  $\Gamma_p$ , of the 154-, 162-, and 376-keV resonances, we use the spectroscopic factors of analog states in the mirror nucleus,  $^{26}\text{Mg}$  [20,39]. For the 414-keV state, we adopt the experimentally determined  $\Gamma_p$  of Ref. [32], while for the level at 432 keV, we assume

TABLE II. Properties of resonant states in the  $^{25}\text{Al}(p, \gamma)$  reaction.

$E_x$ [keV]	$E_r$ [keV]	$J^\pi$	$\Gamma_p$ [eV]	$\Gamma_\gamma$ [eV]	$\omega\gamma$ [eV]
5668	154	$1^-$	$3.1 \times 10^{-7}$	0.26 <sup>a</sup>	$7.8 \times 10^{-8}$
5676	162	$1^+$	$< 8.9 \times 10^{-9}$	0.12 <sup>a</sup>	$< 2.2 \times 10^{-9}$
5890	376	$0^+$	0.004	0.009 <sup>a</sup>	$2.4 \times 10^{-4}$
5928	414	$3^+$	2.9	0.040	0.023
5946	432	$(4^+)$	0.007 <sup>b</sup>	0.024 <sup>a</sup>	0.004

<sup>a</sup>Based on shell-model calculations with the SPDPF interaction.

<sup>b</sup>Assuming  $\ell = 2$  capture and  $C^2S = 0.015$  [35].

$\ell = 2$  capture and a shell-model calculated spectroscopic factor  $C^2S = 0.015$  [35]. At temperatures  $T > 0.25$  GK, we find that the key  $3^+$  resonance at 414 keV remains the dominant contributor to the  $^{25}\text{Al}(p, \gamma)$  stellar-reaction rate, as shown in Fig. 6. The newly identified  $1^-$ , 154-keV resonance increases the stellar reaction rate by an order of magnitude for a temperature of  $T = 0.2$  GK and entirely governs the reaction at cooler temperatures. At 0.2 GK the timescale for proton capture on  $^{25}\text{Al}$  is now comparable with that for its  $\beta^+$  decay, in contrast to earlier work, e.g., Ref. [50]. Furthermore, at a temperature of 0.16 GK, the temperature achieved at the base of the envelope of a SAGB star, our new  $^{25}\text{Al}(p, \gamma)$  reaction rate is a factor  $\approx 50$  higher than previous estimates due to the new  $1^-$  resonance. However, the significantly lower densities in AGB stars, compared to novae, mean that it is very unlikely that the  $^{25}\text{Al}(p, \gamma)$  reaction is active in these environments.

To assess the astrophysical implications of the present work, we have performed a series of nova-outburst simulations using the hydrodynamic, Lagrangian, time-implicit code SHIVA [51,52]. Energy generation by nuclear reactions is calculated using a network of 120 nuclear species from  $^1\text{H}$  to  $^{48}\text{Ti}$  linked through 630 nuclear processes. Reaction rates are

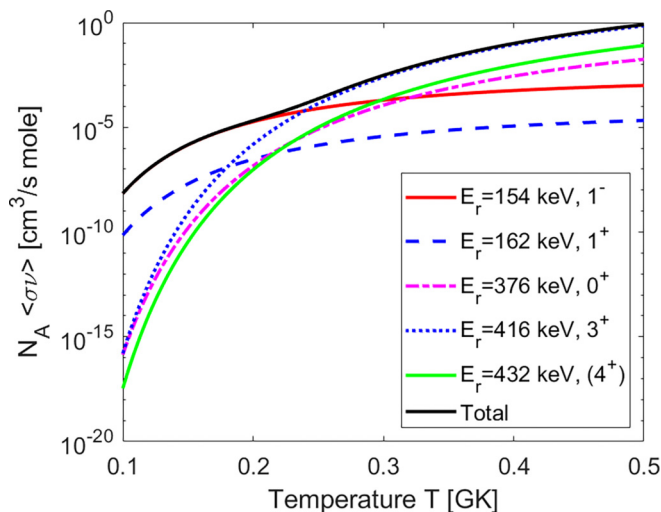


FIG. 6. The  $^{25}\text{Al}(p, \gamma)^{26}\text{Si}$  reaction rate estimated for temperatures up to 0.5 GK assuming the resonance properties presented in Table II and discussed in the text. The contributions of individual resonances to the total rate are also shown.

TABLE III. Mean composition of nova ejecta (in mass fractions,  $X$ , of the total ejected mass,  $M_{ej}$ , for Mg–Si isotopes) from models of nova explosions on 1.15, 1.25, and 1.35  $M_\odot$  ONe white dwarfs. A comparison of high and low rates for the  $^{25}\text{Al}(p, \gamma)$  reaction showed a less than 10% variation in  $^{26}\text{Al}$  yields. As such, we have chosen to only report yields for the present recommended rate of the  $^{25}\text{Al}(p, \gamma)$  reaction.

White dwarf mass	1.15 $M_\odot$	1.25 $M_\odot$	1.35 $M_\odot$
$M_{ej}$ ( $10^{28}$ g)	4.90	3.77	0.90
$X(^{24}\text{Mg})$	$1.55 \times 10^{-4}$	$1.02 \times 10^{-4}$	$0.86 \times 10^{-4}$
$X(^{25}\text{Mg})$	$3.49 \times 10^{-3}$	$2.26 \times 10^{-3}$	$2.45 \times 10^{-3}$
$X(^{26}\text{Mg})$	$3.13 \times 10^{-4}$	$1.79 \times 10^{-4}$	$1.47 \times 10^{-4}$
$X(^{26}\text{Al})$	$9.69 \times 10^{-4}$	$5.68 \times 10^{-4}$	$4.93 \times 10^{-4}$
$X(^{27}\text{Al})$	$8.41 \times 10^{-3}$	$4.48 \times 10^{-3}$	$3.13 \times 10^{-3}$
$X(^{28}\text{Si})$	$5.01 \times 10^{-2}$	$5.40 \times 10^{-2}$	$3.13 \times 10^{-2}$
$X(^{29}\text{Si})$	$0.65 \times 10^{-3}$	$1.29 \times 10^{-3}$	$2.40 \times 10^{-3}$
$X(^{30}\text{Si})$	$0.11 \times 10^{-2}$	$0.58 \times 10^{-2}$	$1.53 \times 10^{-2}$

from the STARLIB database [53], and we have considered accreting 1.15-, 1.25-, and 1.35- $M_\odot$  white dwarfs (with initial luminosity  $10^{-2} L_\odot$  and mass-accretion rate  $2 \times 10^{-10} M_\odot$  per year). Nucleosynthetic yields of Mg–Si isotopes obtained using the current  $^{25}\text{Al}(p, \gamma)^{26}\text{Si}$  reaction rate are displayed in Table III. We find negligible differences in the predicted  $^{26}\text{Al}$  yields due to present uncertainties in the  $^{25}\text{Al}(p, \gamma)^{26}\text{Si}$  stellar reaction rate. In fact, even if the rate of the  $^{25}\text{Al}(p, \gamma)^{26}\text{Si}$  reaction is artificially increased by a factor of 10 the  $^{26}\text{Al}$  yields for 1.15  $M_\odot$  white dwarfs (the most abundant novae) are only reduced by  $\approx 6\%$ . In addition, yields of  $^{26}\text{Mg}$  are only increased by  $\approx 14\%$  in this scenario.

This discussion was based on a  $1^-$  spin-parity assignment for the new 154-keV resonance and hence it being populated in  $\ell = 1$  capture. However, even if the 154-keV resonance has  $J^\pi = 2^+$ , and hence corresponds to  $\ell = 0$  capture in the  $^{25}\text{Al}(p, \gamma)$  reaction (which we consider unlikely, as discussed previously), the reaction rate is only increased by a factor  $\approx 8$  at 0.2 GK and, therefore, the  $^{26}\text{Al}$  yield from novae is reduced by less than 6%. In the event of a  $1^+$  assignment, the 154-keV resonance is populated in  $\ell = 2$  capture the state’s impact on the reaction rate is decreased.

Consequently, we conclude that any variation of the  $^{25}\text{Al}(p, \gamma)^{26}\text{Si}$  rate within its current uncertainties only has a minor impact on the nucleosynthesis of  $^{26}\text{Al}$  in classical novae and that the reaction itself should now be considered well constrained in such environments.

To investigate the overall contribution of classical novae to the observed galactic abundance of  $^{26}\text{Al}$ , we have incorporated the binary stellar evolution code BINARY\_C [54], which includes updated yields from the present SHIVA calculations, with the galactic chemical evolution code L-GALAXIES 2020 [55,56]. L-GALAXIES 2020 is a cosmological scale semianalytic model of galaxy evolution, which runs on the halo merger trees generated from  $N$ -body simulations of dark matter structure formation (in this case, MILLENNIUM-I [57]). By selecting a sample of Milky Way analog (MWA) galaxies in the simulation, we estimate that classical novae are only likely

to be responsible for a maximum contribution of  $\approx 0.2 M_{\odot}$  to the observed active abundance of  $^{26}\text{Al}$  in our galaxy.

On the other hand, these simulations indicate that AGB stars may be responsible for producing up to  $\approx 0.6 M_{\odot}$  of  $^{26}\text{Al}$ , using AGB metal yields from Ref. [58]. This is significantly higher than previously expected and we encourage further investigations on the nucleosynthesis of AGB stars which incorporate new experimental information on reactions relevant to the synthesis of  $^{26}\text{Al}$  in these environments, e.g.,  $^{25}\text{Mg}(p, \gamma)$  [59].

## V. CONCLUSIONS

In summary, we have performed a detailed  $\gamma$ -ray spectroscopy study of the nucleus  $^{26}\text{Si}$ . We observe several high-energy  $\gamma$  rays including a 5667-keV direct-to-ground state transition that most likely corresponds to the decay of the  $1_1^-$  excited level. This newly identified state corresponds to a 154-keV resonance in the  $^{25}\text{Al}+p$  system and, based on an evaluation of the rate, provides the dominant contribution to the  $^{25}\text{Al}(p, \gamma)$  reaction over the temperature range  $T \approx 0.1\text{--}0.2$  GK. Somewhat surprisingly, despite an order of magnitude increase in the reaction rate at lower temperatures in comparison with earlier work, we find that the expected ejected abundance of  $^{26}\text{Al}$  from classical novae remains largely unaffected despite the timescales for proton capture on  $^{25}\text{Al}$  and its  $\beta^+$  decay being comparable at 0.2 GK.

In fact, even with an artificial increase in the  $^{25}\text{Al}(p, \gamma)^{26}\text{Si}$  reaction rate by a factor of 10 we find that the  $^{26}\text{Al}$  yields are only reduced by 6% (for novae involving  $1.15 M_{\odot}$  white dwarfs) leading to the conclusion that this reaction is now sufficiently well constrained to be used in models which estimate the galactic abundance of  $^{26}\text{Al}$ . Using the galactic chemical evolution code, L-GALAXIES 2020, we estimate that classical novae contribute up to a maximum of  $\approx 0.2 M_{\odot}$  to the observed galactic abundance of  $^{26}\text{Al}$  with AGB stars producing up to  $\approx 0.6 M_{\odot}$ .

## ACKNOWLEDGMENTS

United Kingdom personnel were supported by the Science and Technologies Facilities Council (STFC). J.H. acknowledges support under UKRI Future Leaders Fellowship MR/T0222641/1. J.J. acknowledges support from Spanish MINECO Grant No. PID2020-117252GB-I00, the E.U. FEDER funds, and AGAUR/Generalitat de Catalunya Grant No. SGR-661/2017. This research used resources of ANL's ATLAS facility, which is a DOE Office of Science User Facility. Research at ANL, UNC, TUNL, and ORL is supported by Grants No. DE-AC02-06CH11357 (ANL), No. DEFG02-94-ER40834 (UNC), No. DEFG02-94-ER41043 (TUNL), and No. DE-AC05-00OR22725 (ORNL), US Department of Energy, Office of Science, Office of Nuclear Physics.

- 
- [1] T. Lee, D. A. Papanastassiou, and G. J. Wasserburg, *Geophys. Res. Lett.* **3**, 41 (1976).
- [2] N. Dauphas and M. Chaussidon, *Annu. Rev. Earth Planet Sci.* **39**, 351 (2011).
- [3] T. Lichtenberg, G. J. Golabek, R. Burn, M. R. Meyer, Y. Alibert, T. V. Gerya, and C. Mordasini, *Nat. Astron.* **3**, 307 (2019).
- [4] W. A. Mahoney, J. Ling, A. Jacobson, and R. Lingenfelter, *Astrophys. J.* **262**, 742 (1982).
- [5] R. Diehl, C. Dupraz, K. Bennett, H. Bloemen, W. Hermsen, J. Knödlseder *et al.*, *Astron. Astrophys.* **298**, 445 (1995).
- [6] R. Diehl, H. Halloin, K. Kretschmer, G. G. Lichti, V. Schönfelder, A. W. Strong *et al.*, *Nature (London)* **439**, 45 (2006).
- [7] W. Wang, M. G. Lang, R. Diehl, H. Halloin, P. Jean, J. Knödlseder *et al.*, *Astron. Astrophys.* **496**, 713 (2009).
- [8] R. Diehl, M. Lugaro, A. Heger, A. Sieverding, X. Tang, K. A. Li *et al.*, *PASA* **38**, e062 (2021).
- [9] P. Martin, J. Knödlseder, R. Diehl, and G. Meynet, *Astron. Astrophys.* **506**, 703 (2009).
- [10] C. Iliadis, A. Champagne, A. Chieffi, and M. Limongi, *Astrophys. J. Suppl. Series* **193**, 16 (2011).
- [11] J. José, M. Hernanz, and A. Coc, *Astrophys. J. Lett.* **479**, L55 (1997).
- [12] M. Lugaro, C. L. Doherty, A. I. Karakas, S. T. Maddison, K. Liffman, D. A. García-Hernández, L. Siess, and J. C. Lattanzio, *Meteorit. Planet. Sci.* **47**, 1998 (2012).
- [13] J. H. Kastner and P. C. Myers, *Astrophys. J.* **421**, 605 (1994).
- [14] C. L. Doherty, P. Gil-Pons, L. Siess, and J. C. Lattanzio, *PASA* **34**, e056 (2017).
- [15] A. Weiss and J. W. Truran, *Astron. Astrophys.* **238**, 178 (1990).
- [16] J. W. Truran and M. Livio, *Astrophys. J.* **308**, 721 (1986).
- [17] M. Livio and J. W. Truran, *Astrophys. J.* **425**, 797 (1994).
- [18] A. W. Shafter, *Astrophys. J.* **834**, 196 (2017).
- [19] M. B. Bennett, C. Wrede, K. A. Chipps, J. José, S. N. Liddick, M. Santia *et al.*, *Phys. Rev. Lett.* **111**, 232503 (2013).
- [20] L. Canete, G. Lotay, G. Christian, D. T. Doherty, W. N. Catford, S. Hallam *et al.*, *Phys. Rev. C* **104**, L022802 (2021).
- [21] L. Nittler, C. M. D. Alexander, X. Gao, R. M. Walker, and E. Zinner, *Astrophys. J.* **483**, 475 (1997).
- [22] S. Amari, X. Gao, L. R. Nittler, E. Zinner, J. José, M. Hernanz, and R. S. Lewis, *Astrophys. J.* **551**, 1065 (2001).
- [23] L. Siess and M. Arnould, *Astron. Astrophys.* **489**, 395 (2008).
- [24] M. Bose and S. Starrfield, *Astrophys. J.* **873**, 14 (2019).
- [25] F. Strieder, B. Limata, A. Formicola, G. Imbriani, M. Junker, D. Bemmerer *et al.*, *Phys. Lett. B* **707**, 60 (2012).
- [26] L. Buchmann, M. Hilgemeier, A. Krauss, A. Redder, C. Rolfs, H. Trautvetter, and T. Donoghue, *Nucl. Phys. A* **415**, 93 (1984).
- [27] C. Ruiz, A. Parikh, J. José, L. Buchmann, J. A. Caggiano, A. A. Chen *et al.*, *Phys. Rev. Lett.* **96**, 252501 (2006).
- [28] G. Lotay, A. Lennarz, C. Ruiz, C. Akers, A. A. Chen, G. Christian *et al.*, *Phys. Rev. Lett.* **128**, 042701 (2022).
- [29] D. W. Bardayan, J. C. Blackmon, A. E. Champagne, A. K. Dummer, T. Davinson, U. Greife *et al.*, *Phys. Rev. C* **65**, 032801(R) (2002).
- [30] Y. Parpottas, S. M. Grimes, S. Al-Quraishi, C. R. Brune, T. N. Massey, J. E. Oldendick, A. Salas, and R. T. Wheeler, *Phys. Rev. C* **70**, 065805 (2004).
- [31] D. Seweryniak, P. J. Woods, M. P. Carpenter, T. Davinson, R. V. F. Janssens, D. G. Jenkins, T. Lauritsen *et al.*, *Phys. Rev. C* **75**, 062801(R) (2007).

- [32] P. N. Peplowski, L. T. Baby, I. Wiedenhöver, S. E. Dekat, E. Diffenderfer, D. L. Gay *et al.*, *Phys. Rev. C* **79**, 032801(R) (2009).
- [33] K. A. Chipps, D. W. Bardayan, K. Y. Chae, J. A. Cizewski, R. L. Kozub, J. F. Liang *et al.*, *Phys. Rev. C* **82**, 045803 (2010).
- [34] A. Matic, A. M. van den Berg, M. N. Harakeh, H. J. Wörtche, G. P. A. Berg, M. Couder *et al.*, *Phys. Rev. C* **82**, 025807 (2010).
- [35] W. A. Richter, B. A. Brown, A. Signoracci, and M. Wiescher, *Phys. Rev. C* **83**, 065803 (2011).
- [36] D. T. Doherty, P. J. Woods, D. Seweryniak, M. Albers, A. D. Ayangeakaa, M. P. Carpenter *et al.*, *Phys. Rev. C* **92**, 035808 (2015).
- [37] K. A. Chipps, *Phys. Rev. C* **93**, 035801 (2016).
- [38] P. F. Liang, L. J. Sun, J. Lee, S. Q. Hou, X. X. Xu, C. J. Lin *et al.*, *Phys. Rev. C* **101**, 024305 (2020).
- [39] C. B. Hamill, P. J. Woods, D. Kahl, R. Longland, J. P. Greene, C. Marshall, F. Portillo, and K. Setoodehnia, *Eur. Phys. J. A* **56**, 36 (2020).
- [40] J. F. Perello, S. Almaraz-Calderon, B. W. Asher, L. T. Baby, C. Benetti, K. W. Kemper *et al.*, *Phys. Rev. C* **105**, 035805 (2022).
- [41] L. Canete, A. Kankainen, T. Eronen, D. Gorelov, J. Hakala, A. Jokinen *et al.*, *Eur. Phys. J. A* **52**, 124 (2016).
- [42] M. S. Basunia and A. Hurst, *Nucl. Data Sheets* **134**, 1 (2016).
- [43] B. A. Brown and W. D. M. Rae, *Nucl. Data Sheets* **120**, 115 (2014).
- [44] A. R. L. Kennington, G. Lotay, D. T. Doherty, D. Seweryniak, C. Andreoiu, K. Auranen *et al.*, *Phys. Rev. Lett.* **124**, 252702 (2020).
- [45] A. R. L. Kennington, G. Lotay, D. T. Doherty, D. Seweryniak, C. Andreoiu, K. Auranen *et al.*, *Phys. Rev. C* **103**, 035805 (2021).
- [46] S. Paschalis, I. Lee, A. Macchiavelli, C. Campbell, M. Cromaz, S. Gros *et al.*, *Nucl. Instrum. Methods Phys. Res. A* **709**, 44 (2013).
- [47] D. Weisshaar, D. Bazin, P. Bender, C. Campbell, F. Recchia, V. Bader *et al.*, *Nucl. Instrum. Methods Phys. Res. A* **847**, 187 (2017).
- [48] C. N. Davids, B. Back, K. Bindra, D. Henderson, W. Kutschera, T. Lauritsen, Y. Nagame, P. Sugaithan, A. V. Ramayya, and W. Walters, *Nucl. Instrum. Methods Phys. Res. B* **70**, 358 (1992).
- [49] B. A. Brown and W. A. Richter, *Phys. Rev. C* **74**, 034315 (2006).
- [50] A. Parikh and J. José, *Phys. Rev. C* **88**, 048801 (2013).
- [51] J. José and M. Hernanz, *Astrophys. J.* **494**, 680 (1998).
- [52] J. José, *Stellar Explosions: Hydrodynamics and Nucleosynthesis*, Series in Astronomy and Astrophysics (CRC Press, Boca Raton, FL, 2016).
- [53] A. L. Sallaska, C. Iliadis, A. E. Champang, S. Goriely, S. Starrfield, and F. Timmes, *Astrophys. J. Suppl. Series* **207**, 18 (2013).
- [54] R. G. Izzard, L. M. Dray, A. I. Karakas, M. Lugaro, and C. A. Tout, *Astron. Astrophys.* **460**, 565 (2006).
- [55] B. M. B. Henriques, R. M. Yates, J. Fu, Q. Guo, G. Kauffmann, C. Srisawat, P. A. Thomas, and S. D. M. White, *MNRAS* **491**, 5795 (2020).
- [56] R. M. Yates, C. Péroux, and D. Nelson, *MNRAS* **503**, 4474 (2021).
- [57] V. Springel, S. White, A. Jenkins, C. Frenk, N. Yoshida, L. Gao *et al.*, *Nature (London)* **435**, 629 (2005).
- [58] P. Morigo, *Astron. Astrophys.* **370**, 194 (2001).
- [59] G. Lotay, D. T. Doherty, R. V. F. Janssens, D. Seweryniak, H. M. Albers, S. Almaraz-Calderon *et al.*, *Phys. Rev. C* **105**, L042801 (2022).